Submitted to Fisheries Oceanography 13(6)

An Individual-Based Model of the early life history of mackerel (*Scomber scombrus*) in the eastern North Atlantic, simulating transport, growth and mortality

J. BARTSCH[1*] AND S.H. COOMBS[2]

[1] *COMMSYS – Baumackerweg 9, 27607 Langen, Germany*

[2] *The Marine Biological Association of the United Kingdom, The Laboratory, Citadel Hill, Plymouth, PL1 2PB, United Kingdom*

[*] Corresponding author. Tel.: +49 4743 911058, Fax: +49 4743 911057

E-mail: jo.bartsch@commsys.cux.shuttle.de

Running title: Mackerel IBM

ABSTRACT

The main purpose of this paper is to provide the core description of the modelling exercise within the SEAMAR (Shelf Edge Advection Mortality And Recruitment) programme. An Individual-Based Model (IBM) was developed for the prediction of year-to-year survival of the early life history stages of mackerel (*Scomber scombrus*) in the eastern North Atlantic. The IBM is one of two components of the model system. The first component is a circulation model to provide physical input data for the IBM. The circulation model is a geographical variant of the HAMSOM model (HAMburg Shelf Ocean Model). The second component is the IBM, which is an i-space configuration model in which large numbers of individuals are followed as discrete entities to simulate the transport, growth and mortality of mackerel eggs, larvae and post-larvae. Larval and post-larval growth is modelled as a function of length, temperature and food distribution; mortality is modelled as a function of length and absolute growth rate. Each particle is considered as a super-individual representing 10^6 eggs at the outset of the simulation, and then declining according to the mortality function. Simulations were carried out for the years 1998 – 2000. Results showed concentrations of particles at Porcupine Bank and the adjacent Irish shelf, along the Celtic Sea shelf-edge, and in the southern Bay of Biscay. High survival was observed only at Porcupine and the adjacent shelf areas, and, more patchily, around the coastal margin of Biscay. The low survival along the shelf-edge of the Celtic Sea was due to the consistently low estimates of food availability in that area.

Key words: Individual-based model, mackerel larvae, particle distribution, growth, mortality, distribution of survivors

INTRODUCTION

Natural environmental variability is clearly implicated in fisheries recruitment (e.g. see Cowan and Shaw, 2002), with evidence that its influence is most pronounced during the early life history stages (e.g. Pepin, 1991). It is during this period that marked changes in mortality can occur, for example, due to variations in available food, predation pressure or advection to unfavourable situations. Understanding these processes by "traditional" observational field ecology and correlation techniques is problematical, in the first case due to the range of spatial scales to be included, and in the second because they do not directly address the underlying mechanisms. More recently, mathematical modelling techniques have allowed the representation and simulation of both physical and biological oceanographic processes; this allows examination of complex relationships in a potentially unlimited range of different scenarios.

Various modelling studies have shown the important role of circulation for survival of fish larvae (e.g. Berntsen *et al*., 1994; Bartsch and Coombs, 1997); but in most studies, only the physical environment was considered, the influence of biotic factors not being incorporated. There have been a number of approaches to relating the dynamics of growth and mortality in marine fish to environmental variables (for example, in terms of food availability - Bailey *et al*., 1995 or temperature - Pepin, 1991) but only a few have incorporated such biological attributes (e.g. Werner *et al.,* 1996; Hermann *et al*., 1996). The development of Individual Based Models (IBMs) has provided the ability to account for rare individuals, or rare circumstances affecting a few individuals, which may contribute strongly to determining population strength, or variance in growth and mortality within populations. IBMs have been successfully used in modelling studies of the early life history dynamics of various marine fish species in recent years (Rice *et al*., 1993; Hermann *et al*., 1996; Werner *et al*., 1996 and Werner *et al.*, 2001a) and have an acknowledged potential for advancing our understanding of the recruitment process (DeAngelis and Gross, 1992; Crowder *et al*., 1992; Werner *et al.*, 2001b).

Following this reasoning, the SEAMAR (Shelf Edge Advection Mortality And Recruitment) programme was set-up with EU support to develop and apply an IBM to the early life-stages of mackerel (*Scomber scombrus*) in the eastern North Atlantic. The ultimate aim was to predict, in a hindcast mode, growth and mortality during the planktonic phase of the life history of mackerel.

The north east Atlantic mackerel (*Scomber scombrus*) is a commercially fished stock of around 2-3 million tonnes (Anon., 2001). Spawning starts in February off Portugal and extends progressively around the shelf-edge margin of Biscay and west of the British Isle to end around July in waters to the west of Scotland (Lockwood *et al*., 1981). Extensive egg surveys are carried out every three years for estimates of spawning stock size. Incidental information on the distribution and abundance of the 0-group fish are obtained from winter, bottom trawl surveys. There is considerable information on the egg and larval biology of mackerel in the north east Atlantic (e.g. Solá *et al*., 1994; Valdés *et al*., 1996; Conway *et al*., 1999; Coombs, *et al*., 2001; Hillgruber and Kloppmann, 2001), supplemented by results of studies in the north west Atlantic (e.g. Ware and Lambert, 1985). Little is known of the later post-larval stages, mainly because of practical sampling difficulties due to their greater avoidance ability and patchy distribution.

In the present paper, the SEAMAR modelling scheme and main parameterisations are described, together with results on the simulated drift, growth and survival of eggs, larvae and post-larvae. The purpose is to provide the core description of the modelling exercise. Other papers in preparation consider different aspects of the study, including modelling the regional food concentrations, derivation of the energetics equations for larval growth, validation of growth and mortality against field observations, and comparison of the model output with 0-group survey results and recruitment indices. A preliminary description of growth and transport in the IBM, is provided by Bartsch and Coombs (2001). Details of the derivation of temperature mediation of the logistic growth curve are given in Bartsch (2002). A comprehensive description of the SEAMAR project is provided in the final project report (SEAMAR, 2002) and available on the SEAMAR website (www.ieo.es/seamar/seamar.htm).

MATERIALS AND METHODS

The two components of the model system are the IBM and the circulation model, which are run separately. Before carrying out simulations with the IBM, physical input data need to be provided by the circulation model. The circulation model provides three-dimensional (3D) current fields, 3D temperature and 2D sea surface elevation (SSE) fields at a daily rate. These data are used in the advection and diffusion module as well as in the temperature and egg development module, which are described below. In addition, biological input data for the IBM are provided in terms of egg distributions from field surveys as well as food concentrations derived from a food production model; these data are used in the initial spatial and temporal egg distribution module and in the food distribution module, respectively (see below). The parameterisations in the egg and larval vertical distribution modules are based on field data (see below).

The Circulation Model

A three-dimensional, non-linear, baroclinic, numerical model is used to simulate the circulation of the North Sea and the shelf-edge area and adjacent oceanic regions of the eastern North Atlantic. The circulation model is based on HAMSOM (HAMburg Shelf Ocean Model), which was developed at the Institut für Meereskunde, Hamburg and transferred to the SEAMAR area. Details of the model are given by Backhaus (1985).

The model area extends from 40° 00' N to 63° 20' N and from 24° 30' W to 14° 15' E (Fig. 1). The horizontal grid resolution is 10' of latitude (18.5 km) and 15' of longitude (15.9 km at 55° N). Vertical resolution is to a maximum of 12 layers, the layer depths ranging from 10 m to 25 m in the upper 100 m, and increasing progressively in the deeper layers to a maximum depth of 5000 m. The model is forced by the M_2 tide (sea surface elevation at the open boundaries) and six-hourly wind stress and air pressure fields from ECMWF (European Centre for Medium-Range Weather Forecasting), as well as monthly climatological density fields (Levitus, 1982). The monthly climatological density fields are treated prognostically, but are relaxed towards the climatological monthly mean.

The time step of the circulation model is 20 minutes. Due to the high data storage requirements, the input data for the IBM are provided on a daily basis. In essence, the required parameters, currents (*u*-, *v*-, and *w*-components) as well as their variance, sea surface elevation and temperature, are integrated over two M_2 tidal cycles.

The Individual-Based Model (IBM)

The IBM is composed of a number of physical and biological modules to simulate transport, growth and mortality. It is an i-space configuration model (DeAngelis and Rose, 1992) in which large numbers of individuals are followed as discrete entities (Table 1).

A major problem in an individual-based model, once mortality is included, is that large numbers of individuals are needed at the start of a simulation if these are to be continually eliminated by a mortality function during the course of the simulation. The common solution, this being a continual reduction of the number of individuals in the model, can lead to loss of variation, irregular dynamics and a large sensitivity to the value of the random generator seeds introduced at the start (Scheffer *et al*., 1995). The concept developed within SEAMAR to solve this problem is similar to the super-individual concept developed by Scheffer *et al*. (*op*. *cit*.). Each particle is considered as a super-individual representing a specific number (10^6) of eggs at the outset of the simulation, this number declining according to the mortality function during the course of the simulation.

In principle, all modules of the IBM (see below) may be activated or deactivated, depending on the complexity required. For the simplest case, when the IBM is reduced to a purely physical advection model, only the advection module and the initial spatial and temporal egg distribution module are implemented.

Advection and diffusion modules

In the IBM, the simulations of the drift routes are performed by means of particles (super-individuals) using a Monte-Carlo method (Bork and Maier-Reimer, 1978). In essence, the super-individuals are "marked" water particles representing the fish eggs and larvae, which are introduced into the model area and tracked in time and space domains.

The model area and the horizontal and vertical grid resolution of the IBM are the same as for the circulation model, but with a time step of one hour. The boundary conditions in the transport module (advection and diffusion) prescribe a no-flux condition at closed boundaries (the coast and seabed), whereas the particles may leave the model area at open boundaries.

Conceptually, the current field can be split into a large-scale mean current (u) and a small-scale random fluctuation (u') about this mean, i.e. $U = u + u'$. The small-scale fluctuations are parameterized using the current variance (Backhaus, 1989; Bartsch and Knust, 1994). Thus, during each time step, the particles experience a directional transport by the mean current (advection) as well as a random transport, in both magnitude and direction, by the small-scale fluctuations (diffusion).

Temperature module

In this module, the daily average temperature that each particle encounters on its way through the 3D environment is calculated. The temperature encountered by each particle at each 1-

hourly time step is recorded and the average calculated at the end of the day. The daily temperature is stored to provide temperature histories for each particle.

Initial spatial and temporal egg distribution (ISTED) *module*

The initial spatial and temporal egg distribution (ISTED) module specifies the start date and geographical distribution of the particles (i.e. eggs at spawning). For this purpose, daily egg production data from the 1998 ICES triennial mackerel egg surveys were used (Anon., 1999). These data were spatially and temporally interpolated by a GAM (Generalized Additive Model) to provide weekly input data for the IBM (Beare and Reid, 2002). Data were available from week 5 (29 January) to week 34 (20 – 26 August) and were interpolated from the original 0.5° latitude x longitude resolution onto the IBM grid.

The same 1998 egg distribution data were used for initialization of all simulations examined (i.e. for 1998, 1999 and 2000), since the 1998 survey is the most comprehensive survey carried out to date and no subsequent extensive egg surveys were conducted until 2001.

Egg development and mortality module

The egg development module calculates the time needed for eggs to develop from spawning to hatching, as given by:

$$E = \mathrm{H}/T \tag{1}$$

where E is the egg development time, H is 80 degree-days and T is temperature in °C. This is a close approximation to the formula given by Lockwood *et al.* (1981) based on incubation experiments, but is more amenable to manipulation in conjunction with the temperature module than the original formulation. The temperatures used are the daily averages from the temperature module.

Egg mortalities are set at 10% per day. This estimate is based on experimental results given by Lockwood *et al*. (1977) and Danielssen and Iversen (1977), as well on field observations in the eastern North Atlantic (Thomson, 1989; SEFOS, 1997). Since the duration of egg development is related to the ambient temperatures encountered, this results in slight seasonal and regional differences in cumulative egg mortality.

Egg vertical distribution module

The number of particles per model grid box, obtained from the ISTED module, is distributed vertically in the egg vertical distribution module, which is based on the summary of field sampling results given in Coombs *et al*. (2001). Essentially, the eggs are fairly evenly distributed through the top 200 m of the water column early in the season when there is no thermal stratification, and become progressively restricted to the upper 25 m with development of the seasonal thermocline. An exponential decline function is fitted to the observed egg distributions, with the rate of decline in egg abundance with depth being related to surface temperature (Coombs *et al*., 2001).

Larval vertical distribution and migration module

In this module, the vertical distribution and diel migration of larvae and post-larvae are specified as length and light dependent. A simplified scheme was adopted and applied universally, in which the vertical distribution of mackerel larvae was specified for length classes 0 – 4 mm, 4 – 6 mm, 6 – 8 mm, 8 – 10 mm, 10 – 15 mm and > 15 mm by day and night in 20 m depth bands in the top 60 m of the water column. The scheme was based on results from field sampling, for the larval sizes (i.e. < 10 mm in length), mainly from Hillgruber *et al*. (1997) and for post-larvae (specimens >10 mm in length) as sampled in the current project (SEAMAR, 2002). The switch from day to night-time distributions was based on sunrise and sunset times calculated daily for a position at the centre of the model area.

In summary, the scheme adopted was for the smaller sizes (<10 mm in length) being fairly evenly distributed throughout the 0 - 60 m depth range; for larger sizes (> 10 mm in length), diel migration became progressively more pronounced, with most specimens being at intermediate depths by night (20 – 40 m) and in the surface layer by day (0 – 20 m).

Food distribution module

In the food distribution module, the daily average food concentration encountered by each particle is determined on its passage through the 3D environment. The food concentration at each time step is stored and the average calculated at the end of each day for use in the growth module.

In the absence of sufficient detailed information on the changing spatial and seasonal vertical distribution of food particles, the food concentration data are specified as being vertically homogeneous within the entire depth range of the larvae and post-larvae (the upper 60 m of the water column). The data were computed as weekly fields for the model area for the weeks 3 – 37 (mid January – mid September) for each of the years 1998, 1999 and 2000.

Food concentrations were modelled from egg production rates of representative large (*Calanus*) and small (*Acartia*) copepods, these constituting 39-58% of the diet of larval and post-larval mackerel (Conway *et al*., 1999; Hillgruber *et al*., 1997; Hillgruber and Kloppmann, 2001; SEAMAR, 2002). Based on the formulations given in Prestidge *et al*. (1995), the egg production rates were calculated from the input variables of satellite-derived sea-surface temperature and chlorophyll *a* concentration, providing monthly fields interpolated to weekly averages for each year. Egg production rates per female were raised to population production rates using Continuous Plankton Recorder data (Sir Alistair Hardy Foundation for Ocean Science, Plymouth, UK) and SEAMAR field sampling data on sex ratio and relative abundance of copepodite stages. Finally, production was converted to biomass using published copepod demographics and raised proportionately to total biomass based on the observed fraction of plankton dry weight represented by *Calanus* and *Acartia*.

A full description of the food availability model is given in SEAMAR (2002).

Growth module

In the growth module, the growth rates of larvae and post-larvae are calculated daily as a function of temperature, length and ambient food concentration.

A first analysis of growth from field data sampled on cruises during 1999 showed that a logistic curve was an appropriate approximation of mackerel larval and early post-larval growth (SEAMAR, 2002), using a variable exponential parameter r (Bartsch, 2002):

$$L = L_\infty * (1 + \exp(-r*t + c))^{-1} \tag{2}$$

where L is the length in mm at time t, L_∞ is a constant representing the maximum length attainable in the initial larval and early post-larval growth stanza (set at 80 mm), r is a function of temperature and food concentration (see below), c is the constant of integration, and L=3 mm at time t=0, i.e. at hatch.

The absolute growth rate is a function of length and the exponential parameter r:

$$dL/dt = G = r*L*(1 - (L/L_\infty)). \tag{3}$$

Temperature and food mediation of the parameter r is carried out as follows:

$$r = (r_{opt} - d*(T_{opt} - T)^2)*F_i \tag{4}$$

where r_{opt} is the maximum specific growth rate ($r_{opt} = 0.125$), d is a constant (d=0.00085), T_{opt} is the optimum temperature for growth (19°C), T is the temperature encountered and F_i is a model food index (MFI – see below).

The range of appropriate values for r_{opt} and d depends mainly on the seasonal temperature range and growth rates. Using the available field data, values for the parameters r_{opt} and d were determined in order to provide realistic values of r, i.e. r must remain positive and should tend to some minimum value, r_{min} (Bartsch, 2002), which corresponds to the lowest growth rates observed in the field when substituted into equation (3). The temperature optimum for growth (T_{opt}=19°C) was selected on the basis of the field temperatures likely to be encountered by larval and post-larval mackerel (maximum of around 20°C) and the general energetic consideration that, within the normal ecological range of a species, higher temperatures lead to increased growth rates (see, for example, Otterlei *et al.* (1999) for optimum growth temperature for larval cod, *Gadus morhua*).

The first stage in setting the Model Food Index in equation (4) is calculation of the ratio of available food to the required daily ration for a particular sized larva or post-larva. This is based on a simple energetics model (SEAMAR, 2002) of weight-based daily growth rate, body length, food concentration, light level and food capture efficiency. The numerical value of the ratio varies between 0.00001 and >> 1. Values > 1 are set to unity, as these values denote maximum growth in optimum food concentrations (i.e. food concentrations above which no further food assimilation can be achieved). For use in equation (4), the range of ratio values was linearly re-scaled to give a Model Food Index (MFI) with a range of 0.4 – 1.0. The lower boundary for the MFI was determined from sensitivity tests, such that growth rates from equation (3), using r from equation (4) and substituting MFI=0.4, were not lower than observed in the field during SEAMAR.

A full description of the parameterisation of the food and growth relationship is given in SEAMAR (2002).

For each super-individual in each grid box, the calculated MFI is modified by a random ΔMFI to mimic sub-grid variations in food concentration which are not resolved by the model grid. These random ΔMFI are drawn from a top-hat distribution of width 0.2, which results in a maximum deviation of $\pm$ 0.1 from the calculated MFI for a super-individual per day. Calculated values < 0.4 were set to 0.4. The choice of the numerical value for ΔMFI was based on the requirement to allow sub-grid variation without modifying MFI significantly.

Mortality module

The daily mortality rates of the super-individuals are calculated as a function of length and absolute growth rates. This determines the daily decrease in numbers of the original 10^6 individuals represented by each super-individual. Conceptually, each super-individual can be considered a subset of a cohort. On any day D, $N_{D,i}$ is the number of eggs or larvae represented by each super-individual and is termed the number of "virtual individuals". In essence, $N_{D,i}$ is potentially different for each particle, since egg development time is temperature dependent, growth is temperature and food dependent and mortality is dependent on absolute growth rates and length, and thus implicitly dependent on temperature and food concentration.

The mathematical relationships between growth and mortality have been examined in a number of papers, those of most significance to the present study being Anderson (1988), Beyer (1989), Miller *et al*. (1988), Morse (1989) and Pepin (1991 and 1993). The conclusion is that growth can be used to represent relative survival, since length-specific growth rates and mortality interact to determine survival of a cohort during the pre-recruit period. Based on this, mortality was formulated such that:

1. Absolute growth rates and mortality rates are positively correlated.

2. Mortality rates are inversely correlated with larval length, i.e. mortality decreases as length increases.
3. Cumulative mortality within a specific length range decreases with increasing length.

Additionally, mortality was based on the empirical relationship given by Pepin (1991):

$$M = 5.17 * G^{0.74} L^{-1.17} \tag{5}$$

where G is the absolute growth rate in mm/day and L is length in mm.

The empirical formulation given above is principally similar to an equation of the form:

$$M = c * G^{1-x} / L^{1+x} \tag{6}$$

where c is a constant.

Using daily data over a length range of 3 – 80 mm from the logistic curve for G and L (equations (2) and (3)), a range of sensitivity tests were carried out to find an appropriate value for x in equation (6) which would satisfy the above three criteria. These results showed that x should be ≥ 0.3. A numerical value of $x=0.3$ was selected, as this provided exponential values for G and L which were sufficient for meeting the criteria and closest to their exponential values in equation (5).

Thus, the final formulation for the daily mortality rate in the IBM was:

$$M = 5.0 * G^{0.7} / L^{1.3} . \tag{7}$$

IBM simulations

The final version of the IBM as implemented in the present paper was used to simulate 12 weekly simulations for each of the years 1998, 1999 and 2000. These 12 weeks (week 11 to week 22; 12 March – 3 June) cover the main part of the mackerel spawning season, in which more than 80% of the eggs are spawned (Anon., 1999). Within each of these simulations, data for all i-states (Table 1) were stored daily for the time of the egg phase (6-9 days depending on temperature) and then for a subsequent period of 60 days for the larval and post-larval phases. In order to summarise the extensive output data, they were pooled as follows:

> Time period 1 (T1): All particles released from week 11 to the end of week 16 (12 March – 22 April). This represents the initial spawning period during which ~ 48% of spawning took place, mainly in the Bay of Biscay but also from Porcupine Bank along the Celtic Sea shelf-edge.
>
> Time period 2 (T2): All particles released from week 17 to the end of week 22 (23 April – 3 June). This represents the second part of the spawning period during which ~ 38% of spawning took place. Spawning in the Bay of Biscay is markedly decreased, with peak spawning occurring at Porcupine Bank and adjacent shelf-edge areas.

All particles were released at the mid-week date of each week concerned. For example, during week 11 (12 – 18 March), particles were released on 15 March.

For each yearly simulation, nearly 140000 super-individuals were introduced into the model domain. Due to the spatially and temporally inhomogeneous physical (temperature and currents) and biological (food distribution) environment, all the i-state histories of the super-individuals are potentially different. In order to summarise the regional distribution of lengths reached by the numerous super-individuals at a particular time, the data from the i-states are averaged for each model grid box. Furthermore, since each super-individual represents a different number of virtual individuals, the mean length per super-individual is weighted with respect to the remaining number of virtual individuals represented by each.

It should be noted that the particle and length distributions resulting from the various simulations, do not represent the situation for a specific calendar date, but relate to an elapsed time after their introduction into the model domain (i.e. each weekly input of eggs is followed until 60 days post-hatch and then summed with the other weekly cohorts all at the same age post-hatch).

In order to determine the effect of mortality on the number of virtual individuals and their spatial distribution, the number of virtual individuals represented by each super-individual, at a length of 50 mm, was totalled for all super-individuals within each model grid box. In the case of mortality, a cut-off length needs to be specified, since mortality is formulated as being length-specific and not age-specific. Using an age cut-off would give an incorrect indication of survivors, because longer super-individuals have suffered higher mortality (fewer remaining virtual individuals) over a particular time span, compared to shorter ones which have grown poorly (more remaining virtual individuals). Although using a longer cut-off length would emphasise differences in mortality, a length of 50 mm was chosen as a compromise, so that most super-individuals would reach this length within the 60 day simulation time of larval and post-larval growth. Again, it should be noted that the resultant distributions do not represent the situation for a specific calendar date, but relate to a specific length reached (50 mm) after their introduction into the model domain.

RESULTS

Transport of eggs, larvae and post-larvae

The 1998 GAM egg distribution for time period T1 (i.e. the composite egg distribution for the six weeks of 12 March – 22 April) is shown in Fig. 2a. This represents the starting positions of the particles for the simulations for 1998, 1999 and 2000. Two areas of high egg concentrations are evident, one extending in a band from Porcupine Bank along the Celtic Sea shelf-edge and the other off the north coast of Spain.

Considering the eggs and subsequent larvae/post-larvae as particles only (i.e. no growth and mortality), the resultant distributions at 60 days post-hatch from spawning in time period T1 for 1998, 1999 and 2000, are shown in Fig. 2b,c,d. Common to all of these, is a separation into three areas of concentration, one in the area of Porcupine Bank**,** one along the Celtic Sea shelf-edge, and one in the south eastern Bay of Biscay. During the first part of the spawning season (time period T1) the highest particle concentrations occur consistently in the south eastern Biscay area. Inter annual differences in particle concentrations vary more markedly in the Porcupine and the Celtic Sea shelf-edge areas than for south east Biscay.

Equivalent plots for the initial distribution for time period T2 (23 April – 3 June) and the resultant distribution of particles at 60 days post-hatch for the 1998, 1999 and 2000 simulations, are shown in Fig. 3a-d. The start distribution (Fig. 3a) shows a more northerly location of the Porcupine/Celtic Sea shelf-edge band of concentration and markedly lower numbers in Biscay, compared with the start situation for time period T1 (Fig. 2a). The resultant particle plots (Fig. 3b,c,d) show a similar separation into three areas of concentration, but with lower numbers in the southern Bay of Biscay, consistent with the lower start concentrations in that area, and a more extreme concentration of particles in the area of Porcupine Bank. For time period T2, the inter annual variability of the particle distributions is highest for the Celtic Sea shelf-edge area.

Growth

Regional differences in growth rate are shown in the plots of average length (mm) achieved by super-individuals after 60 days of growth (Figs. 4 and 5). Considering particles released in time period T1 (12 March – 22 April, Fig. 4), a number of similar patterns are seen for all three years of simulation. Two main regions of faster growth (post-larvae reaching lengths of 45 – 70 mm) are evident, compared with three regions of concentration for the particles. One is a northern area, including the area over Porcupine Bank extending onto the Irish Shelf and north westwards, as well as some extension into the edge of the Rockall Trough. The other region is in the south, where there is local variability in the occurrence of areas of faster growth around the coastal margin of Biscay. Outside these two main areas, the lengths achieved are markedly lower, for example, reaching only 20 – 25 mm to the north west of Scotland, and 20 – 30 mm in the Celtic Sea and adjacent shelf-edge area.

Inter annual variations in growth for time period T1 are also evident. For example, the highest growth rates in the northern area were along the western margin of Porcupine Bank in 1999 (Fig. 4b), where they were lowest in 1998 (Fig. 4a), representing a difference in lengths attained of about 15 mm. For the southern area (the shelf margin of Biscay), the highest growth rates are evident for 2000 (Fig. 4c) and lowest in 1998 (Fig. 4a), again with a difference in length attained within 60 days being around 15 mm.

For particles released during time period T2 (23 April – 3 June, Fig. 5), there is a similar separation of faster growing individuals into northern and southern areas, as for particles released in time period T1, but with generally higher growth rates overall (Fig. 5a,b,c). In the northern area, lengths of 60 – 70 mm are usually reached subsequent to release in time period T2, compared with 45 – 55 mm following the T1 release. Additionally, for the T2 release, the area of fast growth extends further north westwards along the shelf and shelf-edge**.** This results in post-larvae reaching lengths of up to 65 mm to the north west of

Scotland, compared with 30 – 40 mm in the same area following the T1 release. For the concentration off the French coast of Biscay, there is less of a contrast in lengths achieved after 60 days, with a range between 70 – 80 mm following the T2 release compared with 60 – 70 mm for T1. For the T2 release, it can also be observed that the growth rates in the Bay of Biscay are considerably higher for the shelf area off the French coast than along the north coast of Spain (Fig. 5).

Inter annual differences in lengths reached after 60 days for the T2 time period, can vary by 10 – 15 mm in the northern area around Porcupine Bank, where a progressive increase in length from 1998 to 2000 is clearly shown (Fig. 5a,b,c). In the south, around the Bay of Biscay, both the progressive annual increase in length and inter annual differences in length were generally less marked than in the north.

Mortality

The combined effects of growth and mortality on survivorship are shown in the distribution plots of remaining numbers of virtual individuals within each model grid box at a length of 50 mm (Figs. 6 and 7).

For particles released during time period T1 (12 March – 22 April), common features for all years (Fig. 6) are the two main regions showing high survival. One of these areas is in the north, centred over the north eastern Porcupine Bank and adjacent Irish Shelf and the other in the south, comprising localised concentrations around the coastal margin of Biscay. Inter annual variability in the distribution of high survival was much less in the northern area than for the more scattered concentrations around the Bay of Biscay.

For releases in time period T2 (23 April – 3 June) there is only one main area of high numbers of surviving virtual individuals (Fig. 7), this being centred over the eastern Porcupine Bank and adjacent Irish Shelf, extending north eastwards along the shelf-edge. In contrast to the 1998 and 1999 distributions, in 2000 higher numbers of survivors also extended southwards from Porcupine Bank along the shelf-edge of the northern Celtic Sea (Fig. 7c). In the south, there were isolated patches of higher numbers of survivors around Biscay, which varied in location from year-to-year; concentrations were always lower than in the northern area.

DISCUSSION

Particle transport

Results from the particle drift simulations show that the northern area of continuous egg concentration from north west of Ireland, through Porcupine and along the shelf-edge of the Celtic Sea, separates into two distinct areas of larval distribution (Figs. 2 and 3). This separation occurs in the vicinity of 51° N, and is a consequence of the divergent current field just south of Porcupine Bank in the upper mixed layer of the water column, as has been observed previously in field investigations (Pingree, 1993; Mohn, 1999).

North of 51° N, eggs and larvae concentrate over Porcupine Bank due to an anti-cyclonic gyre trapped over the bank (Figs. 2 and 3). This recirculation pattern is a consistent phenomenon and is usually only destroyed by strong winds (Mohn *et al*., 2002). The existence of the anti-cyclonic gyre over Porcupine Bank is corroborated by previous modelling studies (Bartsch and Coombs, 1997) and field investigations (Mohn *et al*., 2002). North of Porcupine, the shelf-edge current transports the particles polewards to the west and north of Scotland, as evidenced by the north eastwards trail of particles, especially for the releases in time period T2 (Fig. 3).

South of 51° N, transport of eggs and larvae is generally south eastwards along the shelf-edge. This is consistent with drift buoy tracks (Pingree, 1993) and with the results of a SEAMAR drifter study in 1999 on the outer Celtic Shelf (SEAMAR, 2002). At about 48° N, a strong off-shelf component of the surface current reduces the southwards flow along the shelf-edge. This is evident in the particle plots of Figs. 2 and 3 as the west/south westerly extension of the Celtic Sea shelf-edge concentration, over deeper water to around 47° N.

For the T1 release along the north coast of Spain, the resultant transport is directed polewards along the shelf-edge (Fig. 2), i.e. eastwards at first, and finally north westwards in the inner south eastern Bay of Biscay. In contrast, for the T2 release, when egg concentrations in the south have declined markedly, eggs and larvae off the north coast of Spain remain mostly in the main spawning areas between 5° - 7° W (Fig. 3). The net transport is approximately zero, due to alternating easterly and westerly winds in the upwelling season. This is consistent with observations of the poleward flow along the Iberian Peninsula, which is intermittently modified during the spring/summer upwelling season by westerly winds, resulting in surface currents towards the equator (Haynes and Barton, 1990; Pingree and Le Cann, 1990).

Although model results showing the current pattern to the north of Biscay are consistent with results from various field observations, there is less confidence in the results for areas around the southern Bay of Biscay. This is a consequence of the relatively low horizontal resolution of the circulation model grid due to computational restraints and the extensive model area. Especially on the narrow shelf off the north coast of Spain, with its steep topography, the model results in small, local areas, should be considered with caution.

Growth

In the IBM, growth is dependent on temperature and food distribution, both of which influence the length distributions after 60 days of larval and post-larval growth (Figs. 4 and 5). The regional north-south temperature gradient, which is reflected in the distributions of length when only temperature mediation is employed in the growth parameterisation (Bartsch and Coombs, 2001), is not discernible in Figs. 4 and 5, but is masked by the effect of food distribution. This is especially clear for the area along the shelf-edge margin of the Celtic Sea, where temperatures are generally higher than at Porcupine Bank, but due to lower food levels, growth is consistently lower.

Lengths attained by super-individuals during the first 60 days of larval and post-larval life are generally higher from the T2 release than from T1 for all years (Figs. 4 and 5). This is a consequence of higher temperatures during the growth period following the T2 release compared with T1, as well as the general increase in food concentration. Along the shelf-edge of the Celtic Sea, there is less difference in growth between the two release periods, mostly due to the consistently low food abundance in that area. Along the north coast of Spain and in the south eastern corner of Biscay, lengths are also similar for the two release periods; this is a result of higher food abundance and lower temperature following the T1 release and, conversely, lower food and higher temperatures for the T2 release.

The highest variability in growth rates, and thus lengths attained, is evident over Porcupine Bank from both the T1 and T2 releases (Figs. 4 and 5). This reflects the large increase in food concentrations in this area, by approximately 3 orders of magnitude, and the slow rate of seasonal warming at the beginning of the spawning season, i.e. sensitivity of larval growth to changes in the rate of increase of food concentration.

Distribution of survivors

The mortality of super-individuals is parameterised in terms of length and growth rate and is therefore critically dependent on the parameterisation of growth itself. Growth is mediated by temperature and food availability, both of which are temporally and spatially inhomogeneous over the spawning season. The distribution and evolution of the temperature field is relatively simple. Firstly, there is a general north-south temperature gradient over the entire model area, with warmer temperatures occurring in the south; secondly, temperatures increase progressively over the period of the simulations. The distribution and evolution of the food concentration field is more complex. The important features are that, while there is a general increase in food concentration over the larval and post-larval growth periods, the increase is relatively higher and more sustained from Porcupine northwards than around the Bay of Biscay. Furthermore, in the intermediate region along the shelf-edge of the Celtic Sea, the modelled food concentrations are consistently relatively low.

The conclusion of the combined effects of temperature and food availability on survival, via growth, together with the drift/retention patterns, is in the plots of remaining numbers of virtual individuals (Figs. 6 and 7). For both time periods, the concentration of survivors in the Porcupine area and north eastwards, is mainly due to the influence of high food concentrations, but also to some retention of particles at Porcupine Bank. Conversely, the low numbers of survivors along the Celtic Sea shelf-edge, where there were concentrations of particles, is a reflection of relatively low food availability. The concentration of survivors along the north coast of Spain and on the French shelf from the T1 release, is a result of both high temperatures and moderate food levels relatively early in the season.

Model capabilities

The IBM described here is crucially dependent on a number of factors. One of the most important is the availability of a circulation model to provide the physical input data needed to simulate transport (currents) and growth (temperature). Other essential input data required for the IBM are the initial egg distributions from field surveys, as well as the modelled food concentrations. In addition, field data on the vertical distribution of eggs and larvae are needed in order to parameterise their position in the water column; this is important because the direction of wind induced currents can vary markedly in the near surface layers.

To a large extent, evaluation of the model scheme described here, depends on results from validations against field data. This has been carried out for comparisons of modelled growth against otolith growth data, and for the plots of survival and abundance against 0-

group trawl survey data (SEAMAR, 2002 and papers in preparation). Within the limitations of the otolith data and the different life-stages represented by the model output compared with the 0-group (around 4 months older), the model was justified, but only to the extent that it was not producing unrealistic results. At the same time, it should be recognised that, at the current level of sophistication, the modelling scheme is equally useful as an investigative tool, used, for example, to explore the effects of different climatic scenarios, as for its absolute predictive capability.

Inevitably, in putting together an IBM which ranges from ocean basin scale circulation to the energetics of larval feeding, there are weaknesses. Some aspects, such as the model scale or selection of the circulation model employed, can be easily enhanced or substituted. Others, such as parameterisation of larval feeding and growth, require intensive experimental programmes for definitive improvements. Implementation of the food model is also clearly a simplification but is one of the few attempts to incorporate an explicitly modelled prey field (e.g. comparable to the NPZ production model used in the IBM of Herman *et al.*, 2001) in an IBM. This advances on the use of static prey fields (e.g. Werner *et al.*, 2001a) or of using temperature as a proxy for environmental factors (Heath and Gallego, 1996).

ACKNOWLEDGEMENTS

This work has been supported by EU contract FAIR-CT98-3695. The authors acknowledge the collaborative input throughout of all other participating scientists at the following laboratories: MBA, Plymouth, UK; PML, Plymouth UK; IEO, Santander, Gijon, Malaga and Madrid, Spain; IHF, Hamburg, Germany; AZTI, San Sebastian, Spain; MLA, Aberdeen, UK; NUI, Galway, Eire; IPIMAR, Lisbon, Portugal; BAH/AWI, Bremerhaven, Germany; CEFAS, Lowestoft, UK; HYDROMOD, Wedel, Germany.

REFERENCES

Anderson, J.T. (1988) A review of size dependent survival during pre-recruit stages of fishes in relation to recruitment. *J. Northw. Atl. Fish. Sci.* **8:**55-66.

Anon. (1999) Report of the Working Group on Mackerel and Horse Mackerel Egg Surveys. *ICES C.M. 1999/G:5.*

Anon. (2001) Report on the Working Group on the assessment of mackerel, horse mackerel, sardine and anchovy. *ICES C.M. 2001/ACFM:6.*

Backhaus, J.O. (1985) A three-dimensional model for the simulation of shelf sea dynamics. *Dt. hydrogr. Z.* **38:**165-187.

Backhaus, J.O. (1989) On the atmospherically induced variability of the circulation of the Northwest European shelf sea and related phenomena. In: *Modeling Marine Systems.* A. M. Davies (ed.). CRC Press Inc., Boca Raton, Florida, pp. 93–134.

Bailey, K.M., Canino, M.F., Napp, J.M., Spring, S.M. and Brown, A.L. (1995) Contrasting years of prey levels, feeding conditions and mortality of larval walleye pollock *Theragra chalcogramma* in the western Gulf of Alaska. *Mar. Ecol. Prog. Ser.* **119:**11-23.

Bartsch, J. (2002) Modelling the temperature mediation of growth in larval fish. *Fish. Oceanogr.* **11:**310-314.

Bartsch, J. and Knust, R. (1994) Simulating the dispersion of vertically migrating sprat larvae (*Sprattus sprattus* (L.)) in the German Bight with a circulation and transport model system. *Fish. Oceanogr.* **3:**92-105.

Bartsch, J. and Coombs, S.H. (1997) A numerical model of the dispersion of blue whiting larvae, *Micromesistius poutassou* (Risso), in the eastern North Atlantic. *Fish. Oceanogr.* **6:**141–154.

Bartsch, J. and Coombs, S. (2001) An individual-based growth and transport model of the early life history stages of mackerel *(Scomber scombrus)* in the eastern North Atlantic. *Ecol. Mod.* **138:**127-141.

Beare, D. J. and Reid, D. G. (2002) Investigating spatio-temporal change in spawning activity by Atlantic mackerel between 1977 and 1998 using Generalized Additive Models. *ICES J. mar. Sci.* **59:**711-724.

Berntsen, J., Skagen, D.W. and Svendsen, E. (1994) Modelling the transport of particles in the North Sea with reference to sandeel larvae. *Fish. Oceanogr.* **3:**81-91.

Beyer, J.E. (1989) Recruitment stability and survival – simple size-specific theory with examples from the early life dynamics of marine fish. *Dana* **7:**45-147.

Bork, I. and Maier-Reimer, E. (1978) On the spreading of power plant cooling water in a tidal river applied to the river Elbe. *Advances in Water Resources* **1:**161-168.

Conway, D.V.P., Coombs, S.H., Lindley, J.A. and Llewellyn, C.A. (1999) Diet of mackerel (*Scomber scombrus*) larvae at the shelf-edge to the south west of the British Isles and the incidence of piscivory and coprophagy. *Vie Mil*. **49:**213-220.

Coombs, S.H., Morgans, D. and Halliday, N.C. (2001) Seasonal and ontogenetic changes in the vertical distribution of eggs and larvae of mackerel (*Scomber scombrus* L.) and horse mackerel (*Trachurus trachurus* L.). *Fish. Res*. **50:**27-40.

Cowan, J.H. and Shaw, R.F. (2002) Recruitment. In: *Fishery Science*. L.A. Fuiman & R.G. Werner (eds). Oxford: Blackwell Science, pp. 88-111.

Crowder, L.B., Rice, J. A., Miller, T.J. and Marschall E.A. (1992) Emperical and theoretical approaches to size-based interactions and recruitment variability in fishes. In: *Individual-based models and approaches in ecology: populations, communities and ecosystems.* D.L. DeAngelis & L.J. Gross (eds). New York: Chapman and Hall, pp. 237-255.

Danielssen, D.S. and Iversen, S.A. (1977) The development and mortality of mackerel eggs (*Scomber scombrus* L.) in different temperatures. *ICES C.M. 1977/L:19.*

DeAngelis, D.L. and Gross, L.J. (1992) *Individual-based models and approaches in ecology: populations, communities and ecosystems*. New York: Chapman and Hall, 525 pp.

DeAngelis, D.L. and Rose, K.A. (1992) Which individual-based approach is most appropriate for a given problem? In: *Individual-based models and approaches in ecology: populations, communities and ecosystems.* D.L. DeAngelis & L.J. Gross (eds). New York: Chapman and Hall, pp. 66-87.

Haynes, R. and Barton, E.D. (1990) A poleward flow along the Atlantic coast of the Iberian Peninsula. *J. Geoph. Res.* **95:**11425 – 11441.

Heath, M.R. and Gallego, A. (1996) Bio-physical modelling of the early life stages of haddock, *Melanogrammus aeglefinus*, in the North Sea. *Fish. Oceanogr.* **7:**110-125.

Hermann, A.J., Hinckley, S., Megrey, B.A. and Stabeno, P.J. (1996) Interannual variability of the early life history of walleye pollock near Shelikof Strait as inferred from a spatially explicit, individual-based model. *Fish. Oceanogr.* **5:**39-57.

Hermann, A.J., Hinckley, S., Megrey, B.A. and Napp, J.M. (2001) Applied and theoretical considerations for constructing spatially explicit individual-based models of marine larval fish that include multiple trophic levels. *ICES J. mar Sci.* **59:**1030-1041.

Hillgruber, N. and Kloppmann, M. (2001) Small-scale patterns in distribution and feeding of Atlantic mackerel (*Scomber scombrus* L.) larvae in the Celtic sea with special regard to inter-cohort cannibalism. *Helgol. Mar. Res.* **55:**135-149.

Hillgruber, N., Kloppmann, M., Wahl, E. and Westernhagen, H. von (1997) Feeding of larval blue whiting and Atlantic mackerel: a comparison of foraging strategies. *J. Fish Biol.* **51 (Suppl. A):**230-249.

Levitus, S. (1982) Climatological Atlas of the World Ocean. *NOAA Prof. Paper* **13:**190 pp.

Lockwood , S.J., Nichols, J.H. and Coombs, S.H. (1977) The development rates of *mackerel* (*Scomber scombrus* L.) eggs over a range of temperatures. *ICES C.M. 1977/J:13.*

Lockwood, S.J., Nichols, J.H. and Dawson, W.A. (1981) The estimation of a mackerel (*Scomber scombrus* L.) spawning stock size by plankton survey. *J. Plankt. Res.* **3:**217–233.

Miller, T.J., Crowder, L.B., Rice, J.A. and Marschall, E.A. (1988) Larval size and recruitment mechanisms in fishes: Towards a conceptual framework. *Can. J. Fish. Aquat. Sci.* **45:**1657-1670.

Mohn, C. (1999) Über Wassermassen und Strömungen im Bereich des europäischen Kontinentalrandes westlich von Irland. (On water masses and currents in the region of the European shelf-edge west of Ireland). *PhD Thesis, Univ. of Hamburg, Germany, 133 pp.*

Mohn, C., Bartsch, J. and Meincke, J. (2002) Observations of the mass and flow field at Porcupine Bank. *ICES J. mar. Sci.* **59:**380-392.

Morse, W.W. (1989) Catchability, growth and mortality of larval fishes. *Fish. Bull. US* **87:**417-446.

Otterlei, E., Nyhammer, G., Folkvord, A. and Stefansson, S.O. (1999) Temperature- and size-dependent growth of larval and early juvenile Atlantic cod (*Gadus morhua*): a comparative study of Norwegian coastal cod and northeast Arctic cod. *Can. J. Fish. Aquat. Sci.* **56:** 2099-2111.

Pepin, P. (1991) Effect of temperature and size on development, mortality, and survival rates of the pelagic early life history stages of marine fish. *Can. J. Fish. Aquat. Sci.* **48:**503-518.

Pepin, P. (1993) An appraisal of the size-dependent mortality hypothesis for larval fish: Comparison of a multispecies study with an empirical review. *Can. J. Fish. Aquat. Sci.* **50:**2166-2176.

Pingree, R.D. (1993) Flow of surface waters to the west of the British Isles and in the Bay of Biscay. *Deep Sea Res. II* **40:**369–388.

Pingree, R.D. and Le Cann, B. (1990) Structure, strength and seasonality of the slope currents in the Bay of Biscay region. *J. mar. Biol. Ass. UK* **70:**857 – 885.

Prestidge, M.C., Harris, R.P. and Taylor, A.H. (1995) A modelling investigation of copepod egg production in the Irish Sea. *ICES J. mar. Sci.* **52:**693–703.

Rice, J.A., Miller, T.J., Rose, K.A., Crowder, L.B., Marschall, E.A., Trebitz, A.S. and DeAngelis D.L. (1993) Growth rate variation and larval survival: Inferences from an individual-based size-dependent predation model. *Can. J. Fish. Aquat. Sci.* **50:**133-142.

SEAMAR (2002) Shelf Edge Advection, Mortality And Recruitment. Contract No. CT98-3695, Final Report, May 2002. European Commission, DG XIV, Brussels.

SEFOS (1997) Shelf Edge Fisheries and Oceanography Study. Contract No. CT93-1105, Final Report, May 1997. European Commission, DG XIV, Brussels.

Scheffer, M., Baveco, J.M., DeAngelis, D.L., Rose, K.A. and van Nes, E.H. (1995) Super-individuals a simple solution for modelling large populations on an individual basis. *Ecol. Model.* **80:**161–170.

Solá, A., Lago de Lanzós, A. and Franco, C. (1994) Seasonal occurrence of mackerel and horse mackerel eggs and larvae in the Cantabrian Sea (VIIIc) and Galicia (IXa) from 1990 to 1992. *ICES C.M. 1994/H:4.*

Thompson, A.B. (1989) Mackerel (*Scomber scombrus*) egg mortality: the Western mackerel stock in Biscay and the Western Approaches in 1977, 1980, 1983 and 1986. *J. Plankton Res*. **11:**1297-1306.

Valdés, L., Lago de Lanzós, A., Solá, A., Franco, C., Sánchez, P. and Alvarez, P. (1996) Hake, mackerel and horse mackerel distribution of eggs and larvae in relation to geostrophic circulation in the Bay of Biscay. *ICES C.M. 1996/S:16.*

Ware, D.M. and Lambert, T.C. (1985) Early life history of Atlantic mackerel (*Scomber scombrus*) in the southern Gulf of St. Lawrence. *Can. J. Fish. Aquat. Sci.* **42:**577-592.

Werner, F.E., Perry, R.I., Lough, R.G. and Naimie, C.E. (1996) Trophodynamic and advective influences on Georges Bank larval cod and haddock. *Deep Sea Res. II* **43:**1793–1822.

Werner, F.E., Mackenzie, B.R., Perry, R.I., Lough, R.G., Naimie, C.E., Blanton, B.O. and Quinlan, J.A. (2001a) Larval trophodynamics, turbulence, and drift on Georges Bank: A sensitivity analysis of cod and haddock. *Sci. mar.* **65 (Suppl. 1):** 99-115.

Werner, F.E., Quinlan, J.A., Lough, G. and Lynch, D.R. (2001b) Spatially-explicit individual based modeling of marine populations: a review of the advances in the 1990s. *Sarsia* **86:**411-421.

LEGENDS TO FIGURES

Figure 1. Model area and bathymetry. The 200 m, 1000 m and 2000 m depth contours are shown. SC – Scotland, IR – Ireland, UK – United Kingdom mainland, RT – Rockall Trough, PB – Porcupine Bank, CS – Celtic Sea and BB – Bay of Biscay.

Figure 2. (a) Initial particle distribution for time period T1 (12 March – 22 April), and subsequent distribution of all particles after 60 days of drift for (b) 1998, (c) 1999 and (d) 2000.

Figure 3. (a) Initial particle distribution for time period T2 (23 April – 3 June), and subsequent distribution of all particles after 60 days of drift for (b) 1998, (c) 1999 and (d) 2000.

Figure 4. Regional distribution of the average length (mm) of all particles released in time period T1 (12 March – 22 April) after 60 days of growth and drift, for (a) 1998, (b) 1999 and (c) 2000.

Figure 5. Regional distribution of the average length (mm) of all particles released in time period T2 (23 April – 3 June) after 60 days of growth and drift, for (a) 1998, (b) 1999 and (c) 2000.

Figure 6. Regional distribution of the total remaining virtual individuals within each model grid box at a length of 50 mm from all super-individuals released in time period T1 (12 March – 22 April), for (a) 1998, (b) 1999 and (c) 2000.

Figure 7. Regional distribution of the total remaining virtual individuals within each model grid box at a length of 50 mm from all super-individuals released in time period T2 (23 April – 3 June), for (a) 1998, (b) 1999 and (c) 2000.

Table 1. The i-state specifications used in the IBM.

i-state	Update	Output
Spawning time and location	None - initial data	None – initial data
Vertical egg position	1-hourly	Daily, during egg stage
Egg development time	Daily	Daily, during egg stage
Egg mortality	Daily	Daily, during egg stage
Temperature field at spawning location	None - initial data	Once only
Vertical larval/post-larval position	1-hourly	Daily
Temporal evolution of geographical position	1-hourly	Daily
Temperature field encountered	1-hourly	Daily average
Food concentration field encountered	1-hourly	Daily average
Age	Daily	Daily
Length	Daily	Daily
Absolute growth rate	Daily	Daily
Specific growth rate	Daily	Daily
Mortality rate	Daily	Daily
Remaining number of virtual individuals per super-individual	Daily	Daily

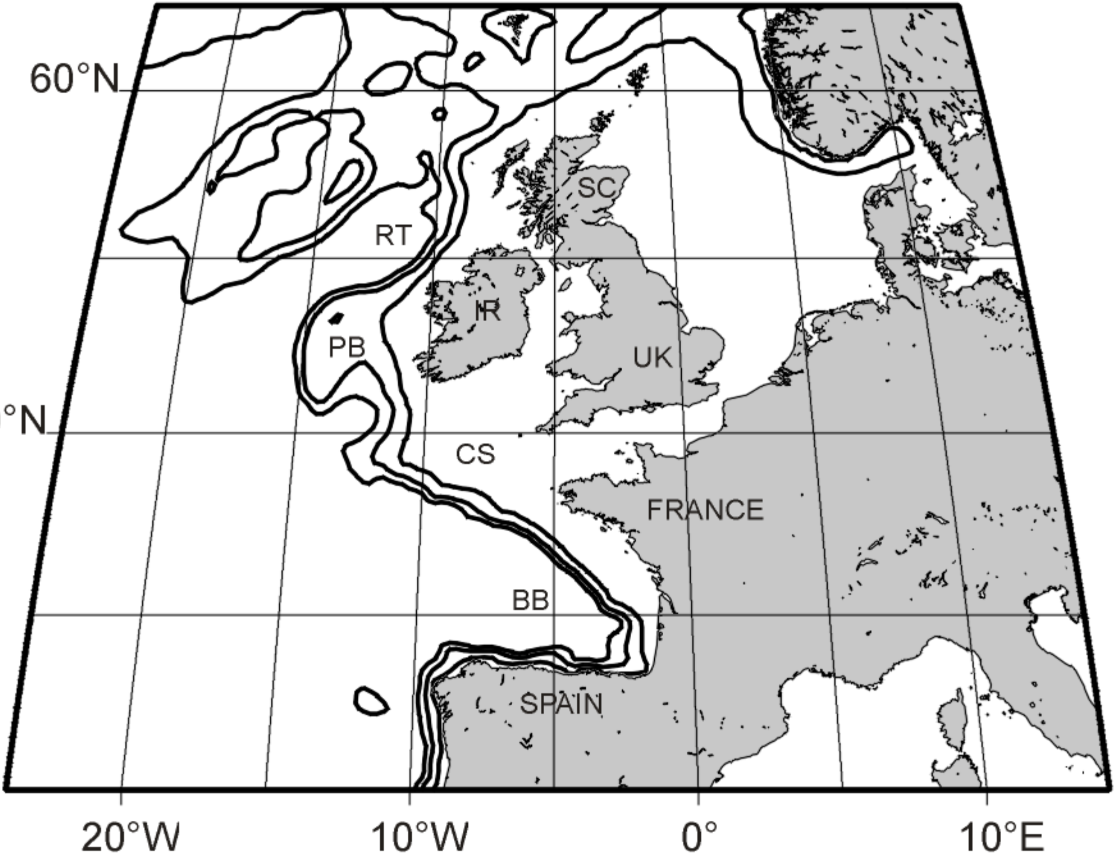
60°N
50°N
20°W
10°W
0°
10°E
RT
SC
IR
PB
UK
CS
FRANCE
BB
SPAIN

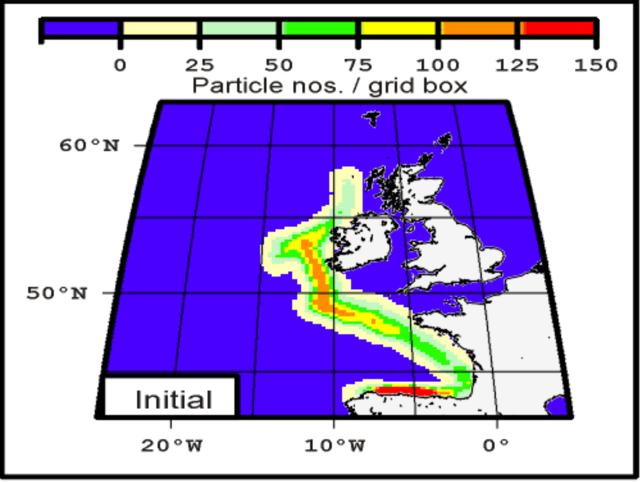
0
25
50
75
100
125
150
Particle nos. / grid box
60°N
50°N
20°W
10°W
0°
Initial

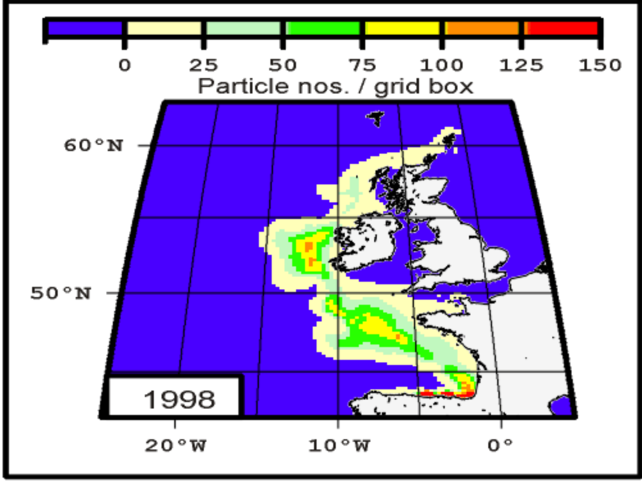
0
25
50
75
100
125
150
Particle nos. / grid box
60°N
50°N
20°W
10°W
0°
1998

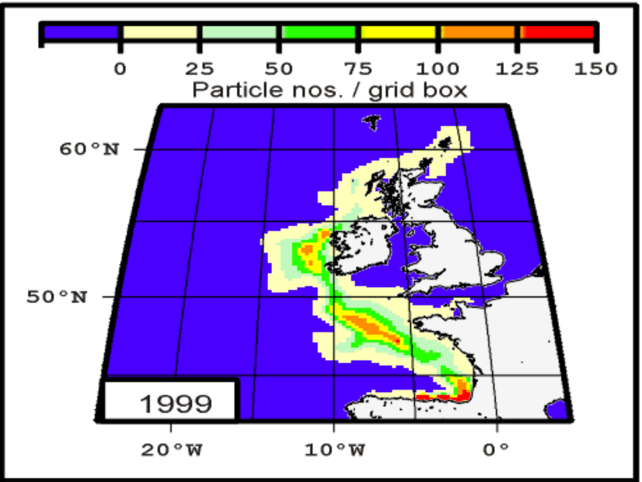
0
25
50
75
100
125
150
Particle nos. / grid box
60°N
50°N
20°W
10°W
0°
1999

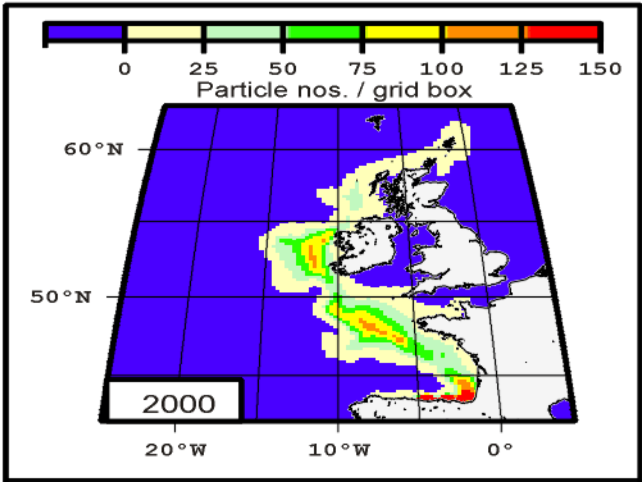
0
25
50
75
100
125
150
Particle nos. / grid box
60°N
50°N
20°W
10°W
0°
2000

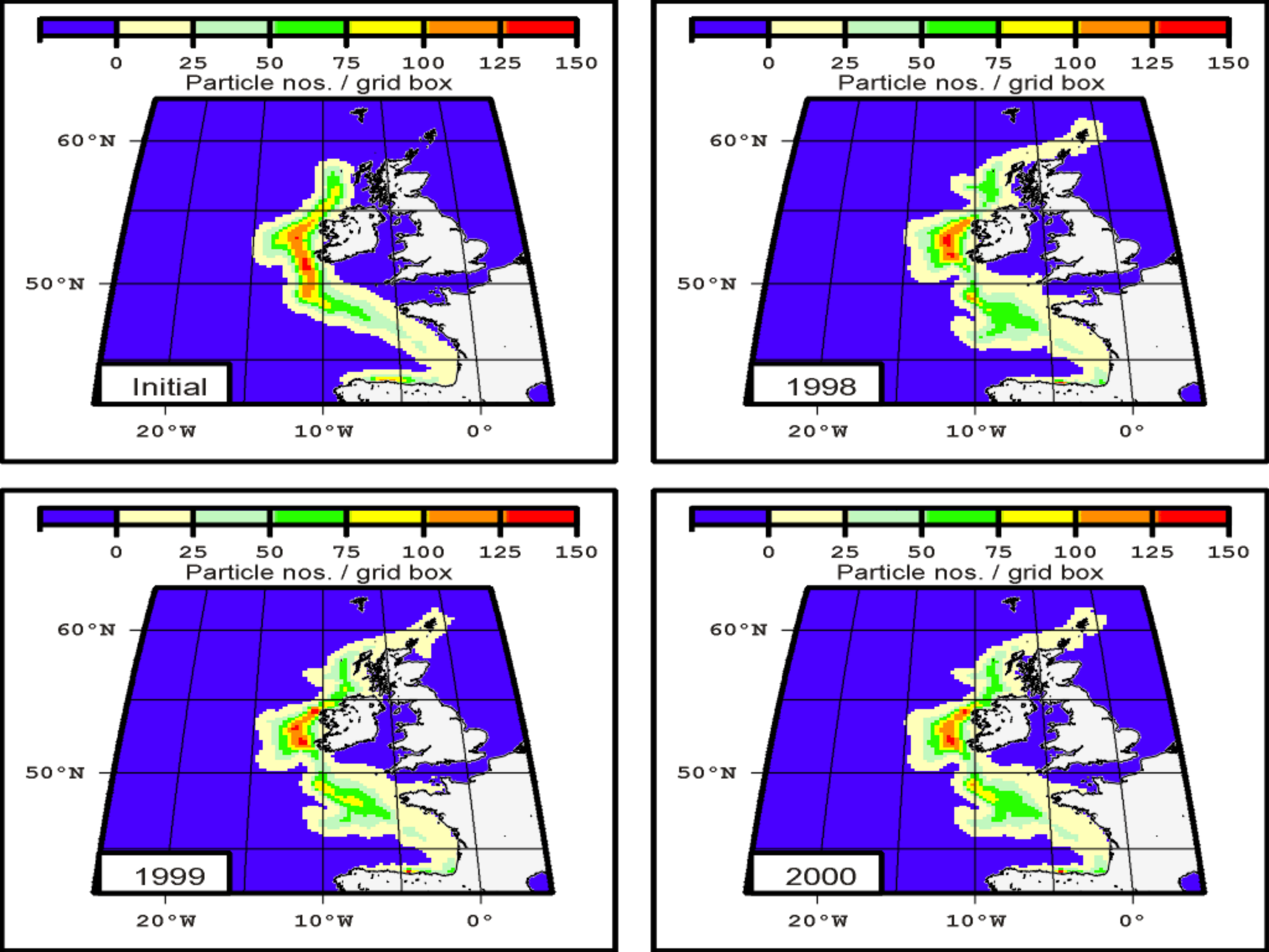
0
25
50
75
100
125
150
Particle nos. / grid box
60°N
50°N
20°W
10°W
0°
Initial
1998
1999
2000

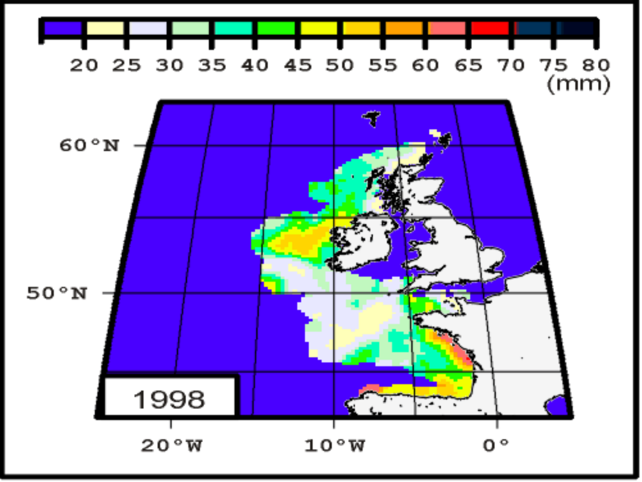
20 25 30 35 40 45 50 55 60 65 70 75 80
(mm)
60°N
50°N
20°W
10°W
0°
1998

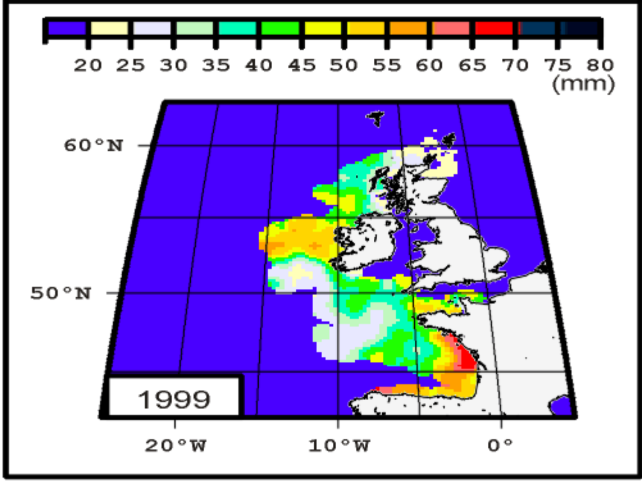
20 25 30 35 40 45 50 55 60 65 70 75 80
(mm)
60°N
50°N
20°W
10°W
0°
1999

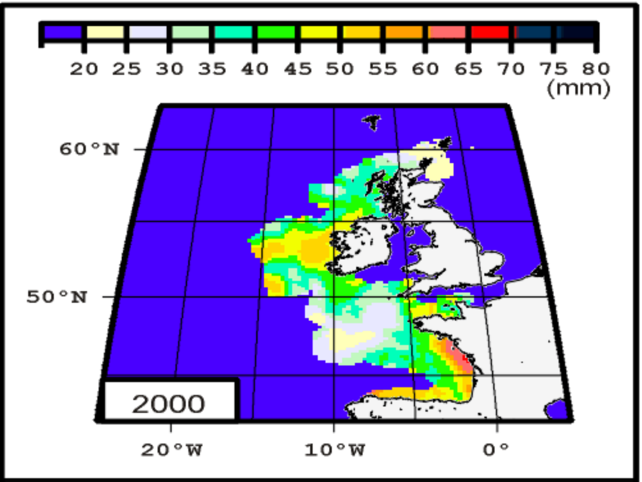
20 25 30 35 40 45 50 55 60 65 70 75 80
(mm)
60°N
50°N
20°W
10°W
0°
2000

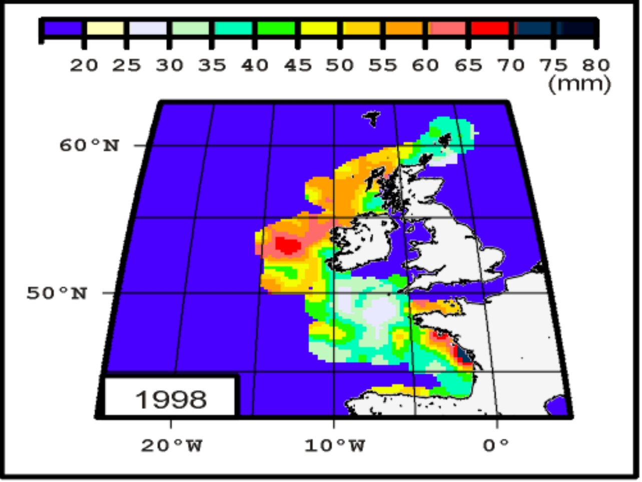
20 25 30 35 40 45 50 55 60 65 70 75 80
(mm)
60°N
50°N
1998
20°W
10°W
0°

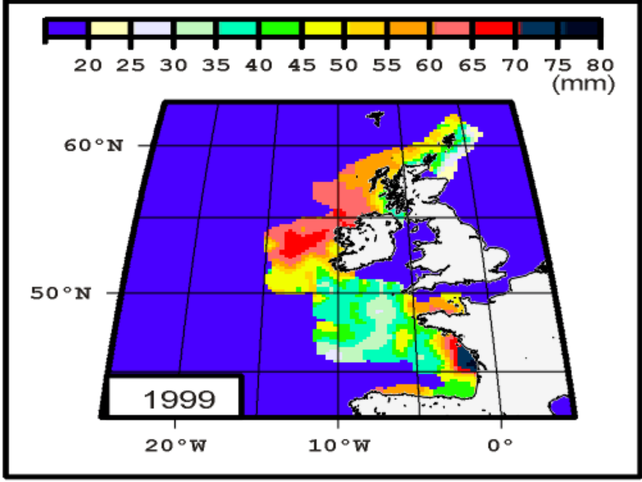
20 25 30 35 40 45 50 55 60 65 70 75 80
(mm)
60°N
50°N
1999
20°W
10°W
0°

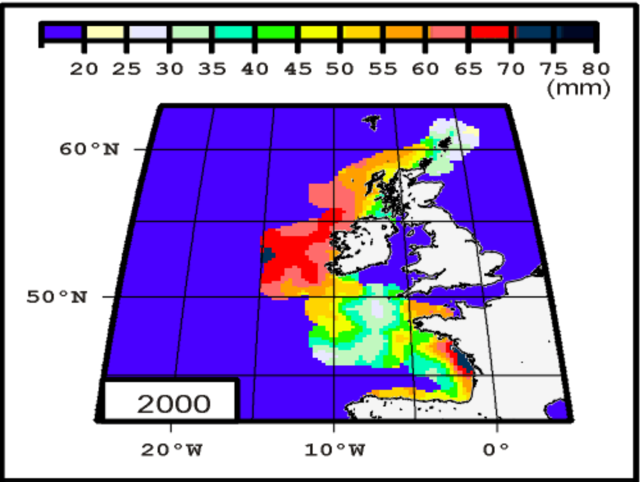
20 25 30 35 40 45 50 55 60 65 70 75 80
(mm)
60°N
50°N
2000
20°W
10°W
0°

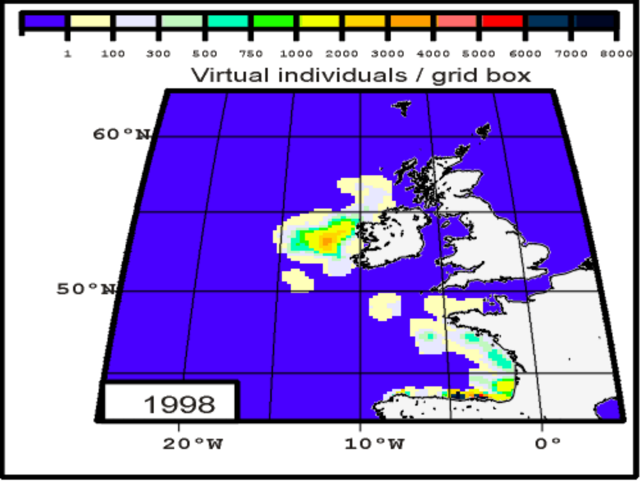
1
100
300
500
750
1000
2000
3000
4000
5000
6000
7000
8000
Virtual individuals / grid box
60°N
50°N
1998
20°W
10°W
0°

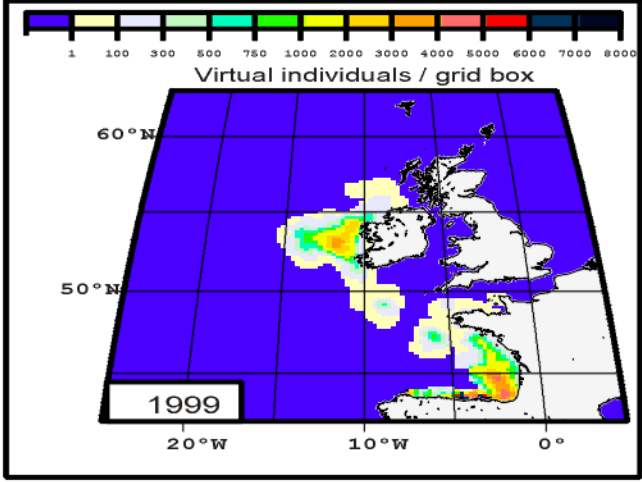
1
100
300
500
750
1000
2000
3000
4000
5000
6000
7000
8000
Virtual individuals / grid box
60°N
50°N
1999
20°W
10°W
0°

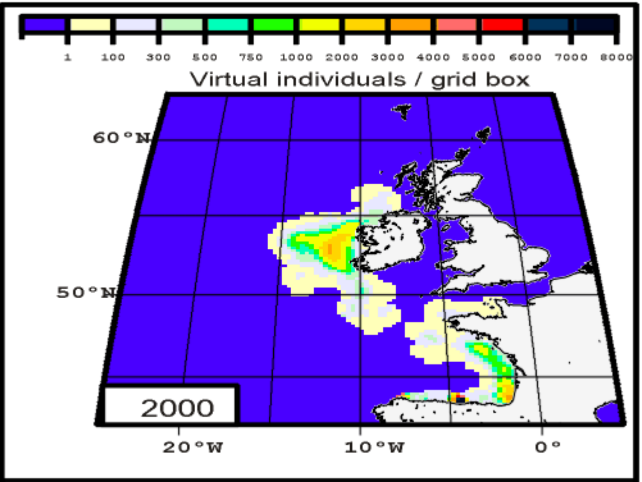
1
100
300
500
750
1000
2000
3000
4000
5000
6000
7000
8000
Virtual individuals / grid box
60°N
50°N
2000
20°W
10°W
0°

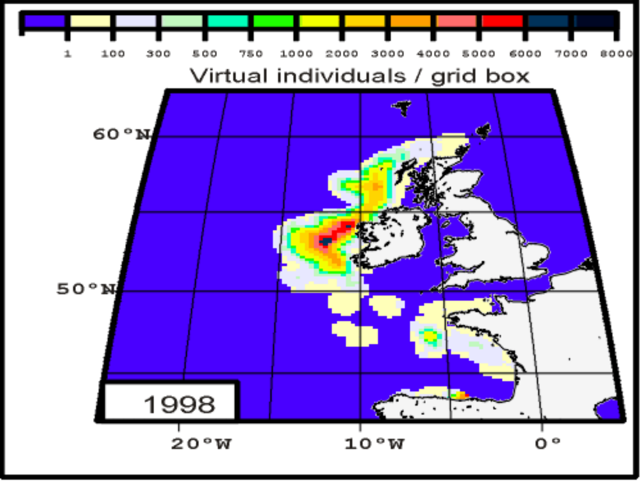
1
100
300
500
750
1000
2000
3000
4000
5000
6000
7000
8000
Virtual individuals / grid box
60°N
50°N
20°W
10°W
0°
1998

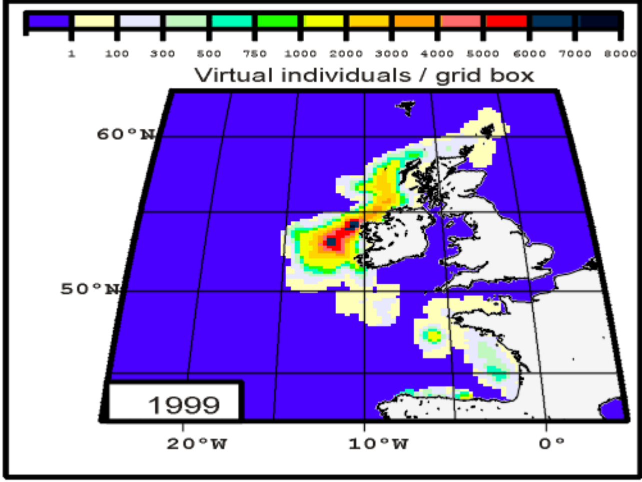
1
100
300
500
750
1000
2000
3000
4000
5000
6000
7000
8000
Virtual individuals / grid box
60°N
50°N
20°W
10°W
0°
1999

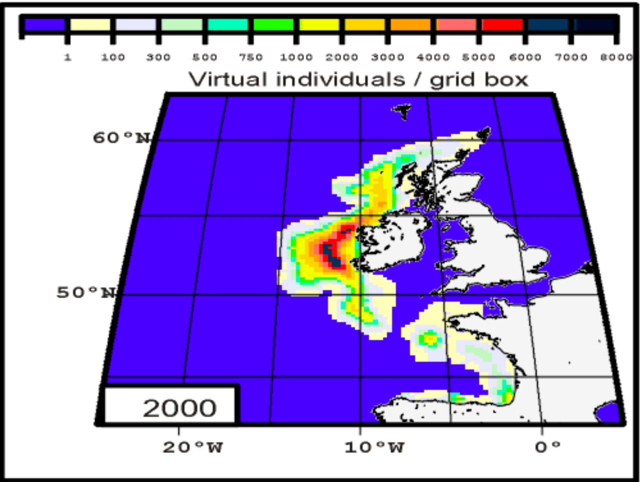
1
100
300
500
750
1000
2000
3000
4000
5000
6000
7000
8000
Virtual individuals / grid box
60°N
50°N
20°W
10°W
0°
2000